# Redundancy optimization strategy for hands-on robotic surgery.

Beatrice Barra, Elisa Beretta, Federico Nessi, Giancarlo Ferrigno, Elena De Momi

***Abstract*— During hands-on cooperative surgery, the use of a redundant robot allows to address encumbrance issues in the Operating Room (OR), which can occur due to the presence of large medical instrumentation, such as the surgical microscope. This work presents a new Null Space Optimization (NSO) strategy to constraint the position of the manipulator's elbow within predefined range of motions, according to the spatial requirements of the specific procedure, also taking into account the physical joint limits of the robotic assistant. The proposed strategy was applied to the 7 degrees of freedom (dof) lightweight robot LWR4+. The performance of the NSO was compared to two state-of-the-art null space optimization strategies, i.e. damped posture and fixed optimal posture, over a pool of three non-expert users in both strict ($20deg$) and negligible ($100deg$) angular encumbrance limitations. The NSO strategy was proved versatile in providing wide elbow mobility together with safe distance from relevant continuity null space boundaries, guaranteeing smooth guidance trajectories. Future works would be performed in order to evaluate the potential feasibility of NSO in a real surgical scenario.**

## I. INTRODUCTION

Hands-on robotics has recently shown to provide many benefits to surgery, enhancing the surgeon's skills in performing the surgical task [1]. In the hands-on cooperative mode, the surgeon manually guides the medical instrument attached at the end-effector of the robotic assistant, which provides increased positional accuracy together with reduced surgeon's fatigue. High maneuverability and compliance of the robotic arm are desirable in order to reduce the user's efforts during the robot guidance [2], [3]. The use of a redundant manipulator, i.e. the same end-effector pose can be reached with multiple joint configurations, can introduce higher system manipulability as well as a wider operational workspace. At the same time, redundancy allows to manage encumbrance issues occuring in a complex environment, such as the surgical Operating Room (OR). Different strategies has already been considered to exploit the redundancy of a robotic arm. The inverse kinematics problem was solved in order to guarantee the maximum dynamic manipolability of the Cartesian task at the contact point [4]. Differently, null space optimization methods were developed for minimizing the effective mass and inertia [3] of the manipulator at guidance contact point. Moreover, the respect of position, velocity and acceleration bounds can be used as a criterion for the redundancy solution [5], where the joints exceeding the imposed constraints are saturated and their effects are compensated by the remaining joints. In particular, a Saturation in the Null Space method [6] is proposed to consider all joint motion constraints in a unified framework. All the strategies presented above do not take directly into account the encumbrance problem, which is very significant in robotic surgery since on the surgical floor collisions with medical instrumentation must be avoided, as well as undesired or uncontrolled contacts with the surgeon itself.

This work presents a versatile and flexible Null Space Optimization (NSO) strategy for hands-on robotic surgery, which directly adresses the encumbrance issues in the OR. The NSO allows to adapt to different spatial requirements for specific surgical procedures, respecting the intrinsic physical joint limitations of the robotic arm.

## II. METHODS

A redundancy optimization strategy was designed and developed for the 7 dof lightweight robot LWR4+ (Kuka, Augsburg, Germany), in order to confine the mobility of the manipulator in a predefined range of motion during hands-on robotic surgery. A Cartesian impedance schema [7] is used to control the pose of the surgical instrument during the manual guidance. As in [2], the hierarchical task prioritization strategy [8] is used to combine the primary task to a joint impedance controller:

$$\tau = \mathbf{K}(\mathbf{q} - \mathbf{q}_{des}) \tag{1}$$

where $\tau$ is the vector of the commanded torques, ($\mathbf{K}$) is the joint stiffness, and ($\mathbf{q}$) and ($\mathbf{q}_{des}$) are the actual and desired joint position respectively.

### *A. Null Space Geometric Model*

The 7 dof LWR4+ robot presents a 1 dof circular null space, mimicking the kinematic of the human arm [9]. As shown in Fig. 1, a null space parameter ($ns$), which describes the position of the manipulator's elbow, is defined as:

$$ns = atan2\left(\frac{\overrightarrow{p_{se}} \cdot \overrightarrow{usin}}{\overrightarrow{p_{se}} \cdot \overrightarrow{ucos}}\right) \tag{2}$$

where $\overrightarrow{p_{se}}$ is the vector from the center of the shoulder to the center of the wrist, $\overrightarrow{p_{sw}}$ is the vector from the center of the shoulder to the center of the wrist, and $\overrightarrow{usin}$ and $\overrightarrow{ucos}$ are computed as:

$$\overrightarrow{usin} = \overrightarrow{z_0} \times \overrightarrow{p_{sw}} \tag{3}$$

*This work was supported in part by EU project ACTIVE FP7 ICT 270460

B. Barra is with Electronics, Information and Bioengineering Department, Politecnico di Milano, Milan 20133, Italy beatrice.barra@mail.polimi.it

E. Beretta, F. Nessi, E. De Momi and G. Ferrigno are with the Neuroengineering and Medical Robotics Laboratory, Electronics, Information and Bioengineering Department, Politecnico di Milano, Milan 20133, Italy {elisa.beretta, federico.nessi, elena.demomi, giancarlo.ferrigno}@polimi.it

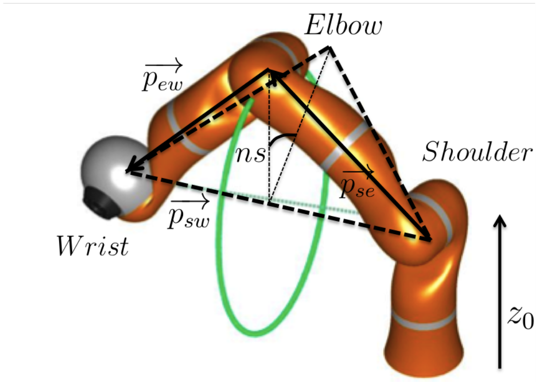


Fig. 1. Representation of the 1 dof circular null space of the LWR4+ robot.

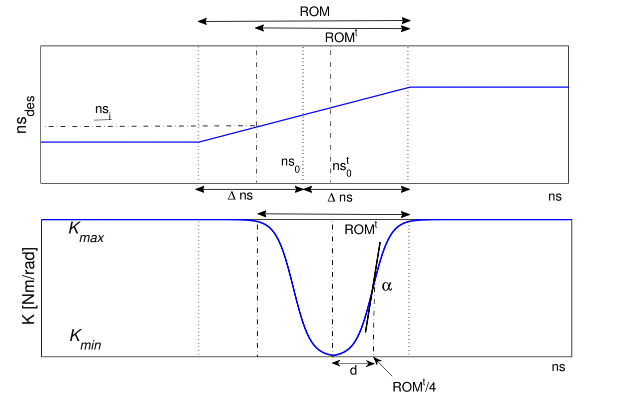


Fig. 2. Modulation of the commanded null space value ($ns_{des}$) and stiffness parameter ($K$). The update of the range of motion $ROM'$ according to the predefined $ROM$ and the minimal continuity constraint ($\bar{ns}_i$) is also reported.

$$\overrightarrow{ucos} = \overrightarrow{p_{sw}} \times \overrightarrow{usin} \tag{4}$$

and $\overrightarrow{z_0}$ is the z axis of the world reference frame. The desired setpoint in the joint space ($\mathbf{q}_{des}$) is computed using the analitic LWR4+ inverse kinematics [9] based on a desired null space value ($ns_{des}$), according to the proposed redundancy optimization strategy.

### B. Null Space Optimization Strategy

The robot mobility in the operating room should address different encumbrance requirements of specific surgical procedures, in order to avoid collisions with other medical instrumentation as well as reducing undesired contacts with the surgeon. The strategy proposed in this work aims to exploits the LWR4+ redundancy to keep the elbow of the manipulator constrainted into a predefined angular range of motion (*ROM*), inside which a certain degree of movement is allowed to provide higher system maneuverability during the guidance of the surgical tool. The ROM is simmetrically defined with amplitude $\Delta ns$ as:

$$ROM = [ns_0 - \Delta ns; ns_0 + \Delta ns]; \tag{5}$$

centered on the initial elbow position $ns_0$.

Inside the *ROM* the motion of the elbow is allowed while it is constrained at the *ROM* extremities. Thus, in order to have a smooth and continuous behavior, the modulation of the null space set point $ns_{des}$ follows the actual $ns$ inside the *ROM* while it is saturated to the limit values at the *ROM* boundaries, as shown in Fig. 2. The joint stiffness $K$ is modulated as a double symmetrical sigmoidal function of $ns$:

$$K = \frac{K_{max} - K_{min}}{1 + e^{\alpha(d - |ns - ns_0|)}} + K_{min} \tag{6}$$

where $K_{max}$ is the maximum value of stiffness, $K_{min}$ is the minimum value of stiffness, $\alpha$ is the curve slope at the inflection point and $d$ is the distance of the inflection point from $ns_0$.

Thanks to those modulations, the impedance control implements a damping and elastic behavior respectively inside and at the bounds of the *ROM*.

### C. Physical Joint Limits Management

Continuity constraints due to the physical joint limits [10] were taken into account in the NSO strategy, because they cause discontinuities in the available $ns$ values, thus possibly leading to unacceptable regions within the predefined ROM. The set of feasible null space values $\Psi_k$ that satisfies the k-th joint limit is described as:

$$\Psi_k = \bigcup_{j=1}^{n_k} \Psi_{kj} \tag{7}$$

where $n_k$ is the number of closed continuous regions $\Psi_{kj}$. In order to satisfy all the joint limits at the same time, the set of globally feasible null space values becomes:

$$\Psi = \bigcap_{k=1}^{7} \Psi_k \tag{8}$$

The initial position $ns_0$ is included in a generic $i^{th}$ interval ($1 < i < n$) among the $n$ discrete continuos intervals associated with the current Cartesian pose. It satisfies the following condition:

$$\underline{ns_i} \leq ns_0 \leq \overline{ns_i} \tag{9}$$

where $\underline{ns_i}$ is the lower bound of the $i^{th}$ continuity interval, and $\overline{ns_i}$ is the upper bound of the $i^{th}$ continuity interval. The range of motion set *a priori* by the user might exceed this interval, trying to get unavailable $ns$ values.

This issue is solved computing for each time step the portion of the predefined range of motion ($ROM^t$) which respects the $i^{th}$ continuity interval for each cartesian pose, according to a safety margin ($\mathrm{d}ns_{sg}$). The boundaries ($\underline{ns}^t$,$\overline{ns}^t$) of the $ROM^t$ are updated as:

$$\underline{ns}^t = \begin{cases} ns_0 - \Delta ns & if \quad \underline{ns_i} + \mathrm{d}ns_{sg} \leq ns_0 - \Delta ns \\ \underline{ns_i} + \mathrm{d}ns_{sg} & else \end{cases} \tag{10}$$

$$\overline{ns}^t = \begin{cases} ns_0 + \Delta ns & if \quad \overline{ns_i} - \mathrm{d}ns_{sg} \geq ns_0 + \Delta ns \\ \overline{ns_i} - \mathrm{d}ns_{sg} & else \end{cases} \tag{11}$$

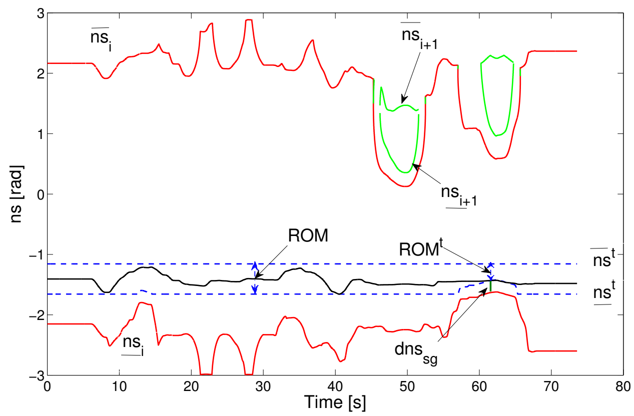


Fig. 3. Example of $ns$ modulation during an assisted guidance. The boundaries of $ROM^t$ ($\underline{ns}^t$, $\overline{ns}^t$) (blue dotted lines) are computed at each time stamp in order to maintain a minimum distance ($dns_{sg}$) from the relevant continuity constraints ($\underline{ns_i}$, $\overline{ns_i}$) (red lines).

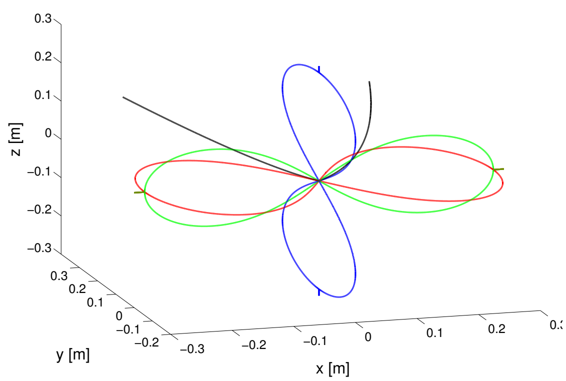


Fig. 4. The trajectory for experimental trials is divided in four parts: a Lemniscate of Bernoulli shaped on the x-y plane (red); a Lemniscate of Bernoulli on the x-z plane (green); a Lemniscate of Bernoulli on the y-z plane (blue); a parabola in a x-y-z plane (black).

An example of the continuity constraints management of the NSO during hands-on guidance is shown in Fig. 3.

### D. Experimental Protocol

To validate the performance of the presented NSO strategy, experimental trials were performed manually guiding the LWR4+ robot along a predefined Cartesian trajectory, composed by ellipsoidal motions on the three planes of the robotic base reference frame, as shown in Fig.4 A comparative assessment was performed between the following strategies:

- A Damped Posture (DP) [2]: a constant damping ($10Nms/rad$) is imposed.
- A Fixed Optimal Posture (FOP) [3]: a constant stiffness ($30Nm/rad$) is imposed on the initial joint configuration, according to $ns_0$.
- The Null Space Optimization (NSO): stiffness is modulated in the range $10-30Nm/rad$ and the safety margin $dns_{sg}$ is set equal to $10deg$. Two hand-on robotic scenarios were considered:

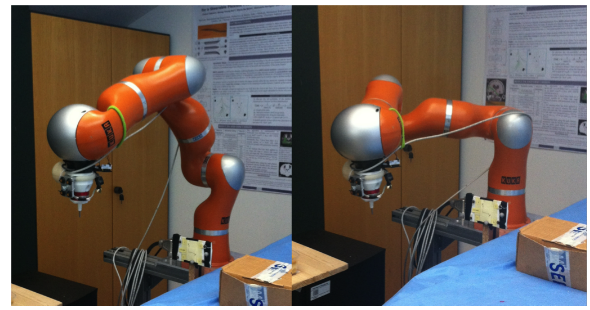

Fig. 5. Initial elbow configurations in the two experimental scenarios: A (left) negligible encumbrance limitations; B (right) strict encumbrance limitations.

1) A: a clinical set-up with negligible encumbrance limitations, e.g. brain mapping in open-skull neurosurgery. The initial joint configuration is with elbow up (Fig. 5a), far away from the physical joint limits. The predefined *ROM* of the NSO is wide ($100deg$).
2) B: a clinical set-up wherein encumbrance specifications are strict due to the presence of large medical instrumentation, e.g. microscopic neurosurgical interventions. The initial joint configuration is with elbow in an horizontal position (Fig. 5b), constrained to be close to the physical joint limits. The predefined *ROM* of the NSO is narrow ($20deg$).

Three non-expert users were asked to perform three trials for each of the redundancy optimization strategy in each clinical scenario.

During each trial the cartesian end-effector pose ($p_{ee}$) was recorded, as well as the current $ns$ value and the effort values at the joints $\tau_e$. The following performance indexes were computed among trials and users:

- *NS range* ($\Delta$), in order to measure the elbow's mobility during the assisted guidance. It was computed as the span of variations on $ns$:

$$\Delta = \max_t \{ns\} - \min_t \{ns\} \tag{12}$$

- *Constraint proximity index* ($\Delta_c$), in order to measure the proximity to the extremities of the elbow mobility due to the joint physical limits. It is computed as the minimum distance of the $ns$ value from the effective continuity boundaries:

$$\Delta_c = \min_t \left\{ (ns - \overline{ns_i}), (ns - \underline{ns_i}) \right\} \tag{13}$$

- *Smoothness index* ($S_j$), in order to evaluate the trajectory smoothness during the assisted guidance. It was computed as the root mean square integral jerk [11], i.e. third discrete time derivative of the end-effector position ($\mathbf{p}_{ee}$):

$$S = \sqrt{\frac{T^5}{L^2} \sum_{i=1}^{N} \left\| \left( \frac{\partial^3 \mathbf{p}_{ee}}{\partial t^3} \right)_i \right\|^2 dt} \tag{14}$$

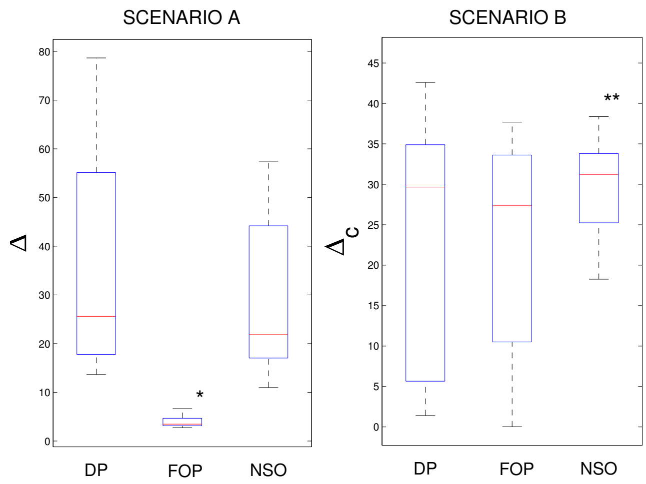


Fig. 6. Experimental results of the *NS Range* ($\Delta$) and *Constraint proximity* ($\Delta_c$) indexes among users and trials for the three null space strategies (DP, FOP, NSO) in the scenario A and B respectively. For each population, the median (red line), 25% and 75% quartiles (blue box), and whiskers (gray dot line) are shown. (*) Statistically significant difference (Kruskal-Wallis test, $p < 0.001$). (**)Statistically significant difference (Bartlett test, $p < 0.05$)

where $N$ is the number of time stamps, $T$ is the total trajectory time and $L$ is the trajectory length.

## III. RESULTS

The null space range index among trials and users for the scenario A, in which the encumbrance constraints are negligible, are reported in Fig. 6. The range of mobility of the FOP mode (median value $\Delta < 5deg$) was confirmed to be significantly (Kruskall-Wallis test, $p < 0.001$) lower with respect to both DP and NSO modes, which resulted with comparable elbow mobility during the assisted guidance (median value $\Delta > 20deg$). Conversely, as shown in Fig. 6, the median proximity index in the scenario B, representing strict encumbrance constraints, resulted comparable among all redundancy strategy (median value of $\Delta_c \in (26,33)deg$, Kruskal-Wallis, $p > 0.8$ ), but the variance was significantly reduced (Bartlett test, $p < 0.05$) with respect to both DP and FOP modes. In fact it has to be noted that all $\Delta$ values of the NSO ($> 15deg$) respects the imposed minimal null space distance from the continuity constraints ($dns_{sg} = 10deg$), differently from the DP and FOP modes, where no strategies are implemented to effectively take into account joint physical limits of the manipulator. As shown in Table I, all three redundancy optimization strategies show comparable smoothness performance ($S < 500$) in both the encumbrance scenarios, except for a smoothness reduction greater than 50% ($S > 1100$) in the case of the DP mode in the scenario B, in which strict constraints are simulated. The normalized mean values respect the smoothness range computed for assisted planar human gestures [11].

## IV. DISCUSSION

Experimental results showed that the NSO strategy was able to adapt to varying encumbrance requirements, simulating different surgical OR conditions, and to combine the positive features of both damped posture [2] and fixed optimal posture modes[3]. In fact, NSO was proved to allow wide mobility of the manipulator's elbow, when encumbrance issues can be neglected (scenario A), such as during brain mapping open-skull neurosurgery. At the same time, NSO was proved to guarantee the respect of strict predefined ROM (scenario B), such as during surgical interventions exploiting other medical instrumentations, e.g. microscopic system, together with time-varying continuity constraints, which are relevant if the manipulator is constrained to work in a configuration close to the physical joint limits.

In this work, the use of the proposed null space optimization strategy was preliminarely proved feasible to address the OR encumbrance issues during hands-on cooperative guidance for robotic surgery. Future work would be performed in order to evaluate the potential versatility and feasibility of the proposed methods in the real surgical scenario with a pool of expert surgeons.

TABLE I
SMOOTHNESS INDEX $S$

| $S$ | DP | FOP | NSO |
|---|---|---|---|
| Scenario A | 482 | 446 | 410 |
| Scenario B | 1140 | 426 | 408 |

## REFERENCES

[1] Davies B, Jakopec M, Harris SJ, Rodriguez y Baena F, Barrett A, Evangelidis A, Gomes P, Henckel J, Cobb J. 2006. Active-constraint robotics for surgery. *Proceeding of the IEEE*, 94(9):1696-1704.
[2] Beretta E, De Momi E, Rodriguexz y Baena F, Ferrigno G. 2015. Adaptive Hands-On Control for Reaching and Targeting tasks in Surgery. *International Journal of Advanced Robotic System*, (accepted).
[3] Petersen J, Rodriguez y Baena F. 2014. Mass and inertia optimization for natural motion in hands-on robotic surgery. *IEEE Int Conf on Intelligent Robots and Systems (IROS2014)*, pp. 4284-4289.
[4] Chiacchio P. 2000. A new dynamic manipulability ellipsoid for redundant manipulators. *Robotica*, 18(4):381-387.
[5] Omrcen D, Zlajpah L,Nemec B. 2007. Compensation of velocity and/or acceleration joint saturation applied to redundant manipulator. *Robotics and Autonomous Systems*, 55(4):337-344.
[6] Flacco F, De Luca A, Khatib O. 2012. Motion Control of Redundant Robots under Joint Constraints: Saturation in the Null Space. *2012 IEEE Int Conf on Robotics and Automation (ICRA2012)*, pp. 285-292.
[7] Albu-Schffer A, Ott C, Hirzinger G. 2004. A passivity based cartesian impedance controller for flexible joint robots - part ii: fullstate feedback, impedance design and experiments. *IEEE Int. Conf. on Robotics and Automation*, 3:2666-2672.
[8] Sentis L, Khatib O. 2005. Synthesis of whole-body behaviors through hierarchical control of behavioral primitives. *International Journal of Humanoid Robotics*, 2(4):505-518.
[9] Wang Y, Artemiadis P. 2013. Closed-Form Inverse Kinematic Solution for Anthropomorphic Motion in Redundant Robot Arms. *Advances in Robotics and Automation*, 2:110.
[10] Shimizu M, Kakuya H, Yoon WK, Kitagaki K, Kosuge K. 2008. Analytical Inverse Kinematic Computation for 7-DOF Redundant Manipulators With Joint Limits and Its Application to Redundancy Resolution. *IEEE Trans on Robotics*, 24(5):1131-1142.
[11] Teulings HL, Contreras-Vidal JL, Stelmach GE, Adler CH. 1997. Parkinsonism reduces coordination of fingers, wrist, and arm in fine motor control. *Experimental neurology*, 146(1):159-170.